Journal of
Micro/Nanolithography,
MEMS, and MOEMS

SPIEDigitalLibrary.org/jm3

# Wavelength selection for multilayer coatings for lithography generation beyond extreme ultraviolet

Igor A. Makhotkin
Erwin Zoethout
Eric Louis
Andrei M. Yakunin
Stephan Müllender
Fred Bijkerk

# Wavelength selection for multilayer coatings for lithography generation beyond extreme ultraviolet

**Igor A. Makhotkin,[a] Erwin Zoethout,[a] Eric Louis,[a] Andrei M. Yakunin,[b] Stephan Müllender,[c] and Fred Bijkerk[ad]**
[a]FOM Institute DIFFER—Dutch Institute for Fundamental Energy Research, Nieuwegein, The Netherlands
[b]ASML, Veldhoven, The Netherlands
[c]Carl Zeiss SMT GmbH, Oberkochen, Germany
[d]University of Twente, MESA+Institute for Nanotechnology, Enschede, The Netherlands
E-mail: I.A.Makhotkin@differ.nl

**Abstract.** The spectral properties of LaN/B and LaN/$B_4C$ multilayer mirrors have been investigated in the 6.5 to 6.9 nm wavelength range, based on measured B and $B_4C$ optical constants. We show that the wavelength of optimal reflectance for boron-based optics is between 6.63 and 6.65 nm, depending on the boron chemical state. The wavelength of the maximum reflectance of the LaN/$B_4C$ multilayer system is confirmed experimentally. Calculations of the wavelength-integrated reflectance for perfect ten-multilayer-mirror stacks show that a B-based optical column can be optimized for a wavelength larger than 6.65 nm.  [DOI: 10.1117/1.JMM.11.4.040501]

Subject terms: multilayer mirrors; next generation extreme ultraviolet lithography photolithography; optical constants; La/$B_4C$; LaN/$B_4C$.

Paper 12081L received Aug. 13, 2012; revised manuscript received Sep. 19, 2012; accepted for publication Sep. 27, 2012; published online Oct. 19, 2012.

## 1 Introduction

Reducing the operating wavelength in advanced photolithography while maintaining the lithography machine's productivity has been a traditional way to enable improved imaging for the last 20 years. The transition from 13.5 nm to 6.5 to 6.9 nm optical lithography offers a possibility to combine high imaging capabilities using a manageable process window.[1] It is shown[2–7] that around 6.6 nm wavelength, the highest reflectance is obtained with multilayer mirrors based on lanthanum as a reflector and boron as a spacer material. Boron is the preferred spacer material for this wavelength because of the close proximity to the boron K-absorption edge.[8,9]

The mirrors for this next generation photolithography require twice shorter bi-layer thickness and approximately four times more layers than Mo/Si mirrors for 13.5 nm extreme ultraviolet lithography (EUVL). The need for a larger amount of periods significantly reduces the optical bandwidth of the multilayer and thus of a 10-mirror La/$B_4C$ based optics: 0.6% compared to 2% for Mo/Si. To enhance the reflectivity of La/B-based multilayers, it might be beneficial to use the technology of contrast enhancement of the interface diffusion barriers similar to that applied in existing 13.5 nm deposition technologies.[10] Currently the measured normal incidence reflectance from real La/B-based multilayers is significantly lower than the theoretically predicted value. One of the factors limiting the reflectance is intermixing at the interfaces between La and B. It has been shown[11] that nitridation of the La layer has a high potential to reduce intermixing due to the formation of the chemically more stable LaN compound.

Key in the design of the next generation EUVL optics will be to match its optimum wavelength to that of the candidate EUV sources based on, for instance, Tb or Gd plasmas. The published emission spectra[12] from these materials show the highest intensities at 6.52 and 6.78 nm, respectively.



Here, we have studied the spectral properties of LaN/B and LaN/$B_4C$ multilayer mirrors by examining the influence of the B and $B_4C$ optical constants on the B-based multilayer reflectivity profile. We confirm the theoretically obtained wavelength dependence of LaN/$B_4C$ mirrors with experimental data and find clear data on EUV-optical properties of candidate materials and optics.

## 2 Application of Measured Optical Constants for Simulation of Multilayer Reflectivity

Calculations of multilayer reflectivity profiles strongly depend on optical constants. The most complete optical constants database in the soft and hard x-ray wavelength range has been published by Henke et. al.[13] and its most updated version can be obtained from the Centre for X-Ray Optics (CXRO) website.[14] The CXRO optical constants for La have been recently updated with experimental values.[15] For boron in the 6.x nm wavelength range, the CXRO optical constants are based on theoretical calculations using the independent atom approximation and can be less accurate, especially in the vicinity of the absorption edge. In addition, possible shifts of the boron absorption edge due to chemical interaction with other species, for example carbon, should be taken into account. The solution to this problem is to use measured B and $B_4C$ optical constants.[16–18]

The wavelength dependencies of the peak intensities calculated for LaN/B and LaN/$B_4C$ multilayer mirrors using measured B and $B_4C$ and CXRO $B_4C$ optical constants are shown in Fig. 1. Here calculations were done for an ideal multilayer model as described in detail in Ref. 19. A significant difference between the CXRO database and measured optical constants is observed around the adsorption edge: the CXRO data shows a steep drop in reflectance for a wavelength below the edge, whereas the use of the measured data results in a more gradual drop in reflectance. Comparing reflectivity profiles of B- and $B_4C$-based multilayers calculated with measured optical constants, we observe a minor shift of the wavelength of maximum reflectance. For LaN/$B_4C$ the maximum reflectivity can be achieved at $\lambda = 6.63$ nm while for LaN/B this maximum

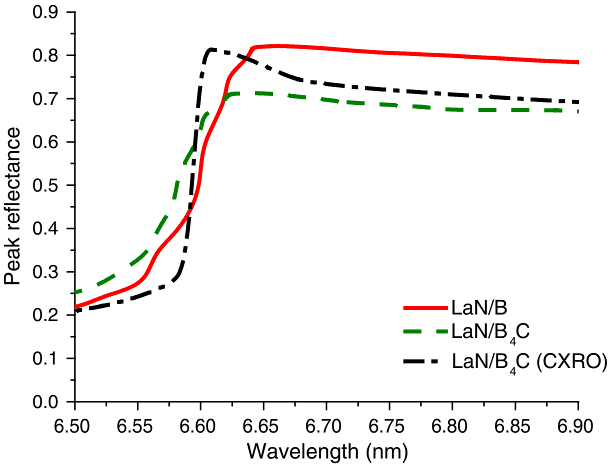


**Fig. 1** Peak reflectivity of a perfect LaN/B multilayer mirror calculated using measured B optical constants (16) (line) and a LaN/$B_4C$ multilayer mirror calculated using measured (17) (dashed) and Henke (13) (dashed-dotted) optical constants.

reflectance is found at $\lambda = 6.65$ nm. This difference can be explained by the 1s B binding energy chemical shift caused by formation of the boron-rich carbide. The most common structure of $B_4C$ contains four $B_{11}C$ icosahedrons and CBC chain as a unit cell,[20–22] while pure crystalline or amorphous boron contains $B_{12}$ icosahedrons.[23] Because of the large variety of possible bonds[20] in $B_4C$, we cannot speak about a well-defined absorption edge position. The total effect of the presence of 20% of C in the boron matrix shifts the onset of photoabsorption of $B_4C$ to higher energies with about 1 eV compared to amorphous and crystalline B.[24] The origin of the B and $B_4C$-based multilayer EUV reflectivity drop at shorter wavelengths is the increase of B absorption. The shift of the absorption onset will lead to the shift of optimal wavelength. Our calculations yielded a difference in the optimal wavelengths of B and $B_4C$ based multilayers of 0.02 nm or ~0.6 in eV, to be compared to the 1 eV shift found above. For estimation of the transmission of an EUV lithography system, we have calculated the integrated reflectivity of the convolution of a system consisting of 10 single-mirror normal incidence mirrors optimized for various wavelengths.

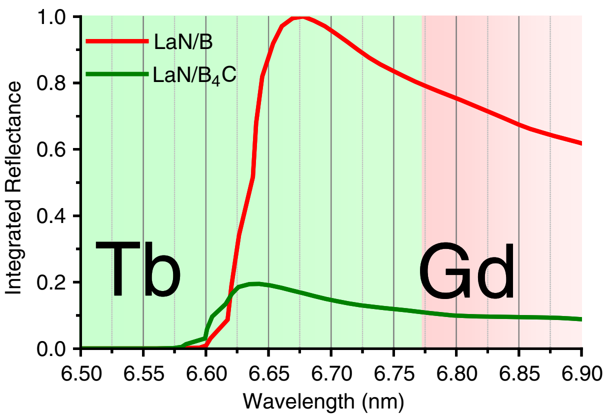


**Fig. 2** Normalized integrated reflectivity for a 10-element mirror system consisting of LaN/B (red) and LaN/$B_4C$ (green) multilayer mirrors, as calculated using measured optical constants for B (16) and $B_4C$ (17). The region of the Tb radiation spectrum is indicated with a green background and of Gd with a red background (12).

In Fig. 2, we show the normalized integrated reflectivity calculated for LaN/$B_4C$ and LaN/B using the measured optical constants in combination with the indication of measured Tb and Gd source spectral regions.[12] All features of the single-mirror peak reflectivity spectra are more pronounced on the 10 mirror integral reflectivity spectra. Figure 2 shows clearly that the wavelength of maximum throughput is at a slightly different wavelength: for the LaN/B material combination, this is at $\lambda = 6.67$ nm while for LaN/$B_4C$ it is at $\lambda = 6.67$ nm. These values are 0.02 and 0.01 nm higher compared to the optimal wavelength of a single B and $B_4C$-based mirror, respectively, because of the influence of the wavelength-dependent bandwidth on the integrated reflectivity.

Comparing the calculated transmission of an LaN/B multilayer coated 10 mirror optical system to the source spectra, we conclude that only the Tb source can be tuned to the optimal wavelength for this multilayer: $\lambda = 6.67$ nm. However, the difference of the optical throughput at $\lambda = 6.67$ nm and $\lambda = 6.8$ nm, where Gd can be used as a source material, is only ~20% for both the LaN/$B_4C$ and LaN/B material combination. That means that the final choice of the wavelength may depend on the relative intensities of Tb and Gd radiation. Another factor, not taken into account in this paper, is the optical design of the lithographic system.

## 3 Normal Incidence EUV Reflectance

To test the influence of the real multilayer structure on the reflectivity profile, 150 period LaN/$B_4C$ multilayer mirrors with different bi-layer thickness ranging from 3.3 to 3.5 nm have been deposited. The period variation allows determining the normal incidence peak reflectivity for the wavelength range from 6.5 to 7.2 nm. The measured maximum reflectivity values for different wavelengths are shown in Fig. 3. The reflectivity has been measured at the radiometry laboratory of the Physikalisch Technische Bundesanstalt (PTB)[25] using synchrotron radiation of the BESSY storage ring in Berlin, Germany. A maximum reflectance of 47.2% is observed at $\lambda = 6.635$ nm. The measured wavelength of maximum reflectivity is in good agreement with the calculated value of a perfect LaN/$B_4C$ mirror described above.

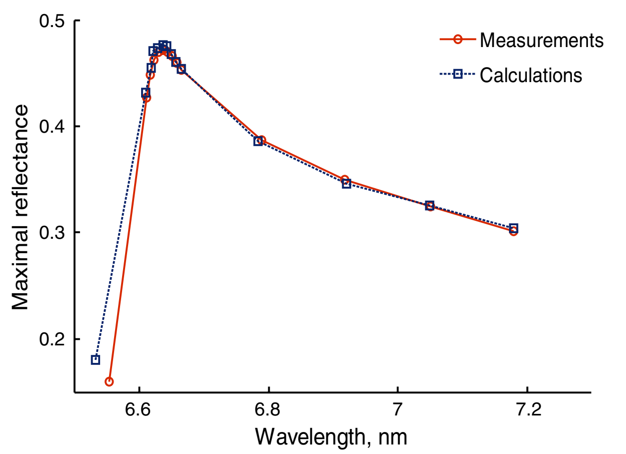


**Fig. 3** Measured and fitted peak reflectivity for a 150 period LaN/$B_4C$ multilayer mirror. The mirror had a lateral gradient in periodicity. The data points represent the maximum reflectance and corresponding wavelength at various positions on the mirror.

To explain the obtained reflectivity, we calculated the reflectance spectrum for each measured multilayer. The thus calculated spectra were fitted to the measurements and the peak reflectance of the fitted spectra is shown in Fig. 3. The model used for these calculations consists of 150 periods of LaN and $B_4C$ layers with different bi-layer thickness for each measured sample. Layer densities and interface roughness were the same for all samples. To have a proper fit of the reflectance dependency on the wavelength in Fig. 3, the La density is reduced to 5 $g/cm^3$, while a $B_4C$ density of 2.5 $g/cm^3$ has been used. The interface roughness, as described by the Debye–Waller factor, equals 0.7 nm for the LaN-on-$B_4C$ interface and 0.4 nm for the $B_4C$-on-LaN interface. Modeling the reflectance profile turns out to be sensitive to the asymmetry of the interfaces but less sensitive to which of the interfaces is the larger one. Finally, for the wavelength region of 6.8 to 7.2 nm, Fig. 3 shows a slope that is steeper than in the calculations for the ideal multilayer represented in Fig. 1. This is explained by the decreased optical contrast due to the lower than bulk density of the La in the LaN layers. Reflectivity improvement requires optimization of the deposition process in order to reduce the interface roughness as well as optimization of the nitridation process. This interface engineering challenge can be solved using reactive or inert ion or plasma treatment during La or $B_4C$ layer deposition or ion/plasma post treatment of deposited layers.

## 4 Conclusions

We have shown that for the evaluation of the performance of LaN/B and LaN/$B_4C$ multilayer optics near the boron K absorption edge, the boron chemical state has to be taken into account. Experimentally determined optical constants were found to properly describe the optical response, as is demonstrated with an experimental verification for a LaN/$B_4C$ multilayer mirror.

The calculated reflectivity of perfect multilayers, i.e., having zero interface roughness, shows that the optimal transmission of a B-based 10-mirror optical system is at a wavelength of 6.67 nm. For a wavelength larger than 6.67 nm there is a slight drop of reflectivity, while for smaller wavelengths the reflectance drops dramatically. Obviously, optimizing the design and fabrication of multilayer mirrors for photolithography systems for wavelengths beyond the current extreme UV requires a trade-off between the multilayer reflectivity response, the eventual source emission and photo resist absorption characteristics, too.

### *Acknowledgments*

This work is part of the project "Multilayer Optics for Lithography Beyond the Extreme Ultraviolet Wavelength Range" carried out with support of the Dutch Technology Foundation (STW). This work is also a part of "Controlling photon and plasma induced processes at EUV optical surfaces (CP3E)" of the Stichting voor Fundamenteel Onderzoek der Materie (FOM) with financial support from the Nederlandse Organisatie voor Wetenschappelijk Onderzoek (NWO), Carl Zeiss SMT, ASML, and the AgentschapNL through the EXEPT program. The authors also would like to express their gratitude to Regina Soufli and Mónica Fernández-Perea from Lawrence Livermore National Laboratory for providing B and $B_4C$ measured optical constants data for our analysis.

### *References*

1. Y. Y. Platonov et al., "Multilayers for next generation EUVL at 6.X nm," *Proc. SPIE* **8076**, 80760N (2011).
2. Y. Y. Platonov, L. Gomez, and D. Broadway, "Status of small d–spacing x–ray multilayers development at Osmic," *Proc. SPIE* **4782**, 152–159 (2002).
3. A. M. Hawryluk and N. M. Ceglio, "Wavelength considerations in soft–x–ray projection lithography," *Appl. Opt.* **32**(34), 7062–7067 (1993).
4. A. V. Vinogradov et al., *Zerkal'naya Rentgenovskaya Optika (X–ray Mirror Optics)*, Mashinostroenie, Leningrad (1989).
5. E. Spiller, *Soft X–ray Optics*, SPIE Optical Engineering Press, Bellingham, WA (1994).
6. T. Tsarfati et al., "Reflective multilayer optics for 6.7 nm wavelength radiation sources and next generation lithography," *Thin Solid Films* **518**(5), 1365–1368 (2009).
7. C. Montcalm et al., "Survey of Ti-, B-, and Y-based soft x-ray-extreme ultraviolet multilayer mirrors for the 2- to 12-nm wavelength region," *Appl. Opt.* **35**(25), 5134–5147 (1996).
8. J. M. Andre et al., "La/$B_4C$ small period multilayer interferential mirror for the analysis of boron," *X–Ray Spectrom.* **34**(3), 203–206 (2005).
9. S. Andreev et al., "Multilayer X–ray mirrors based on La/$B_4C$ and La/$B_9C$," *Tech. Phys.* **55**(8), 1168–1174 (2010).
10. J. Bosgra et al., "Structural properties of sub nanometer thick Y layers in EUV multilayer mirrors," submitted to *J. Appl. Phys.*
11. T. Tsarfati et al., "Nitridation and contrast of $B_4C$/La interfaces and multilayers," *Thin Solid Films* **518**(24), 7249–7252 (2010).
12. S. S. Churilov et al., "EUV spectra of Gd and Tb ions excited in laser–produced and vacuum spark plasmas," *Phys. Scr.* **80**(4), 6 (2009).
13. B. L. Henke, E. M. Gullikson, and J. C. Davis, "X–ray interactions: photoabsorption, scattering, transmission, and reflection at $E = 50–30,000$ eV, $Z = 1–92$," *Atom. Data Nucl. Data* **54**(2), 181–342 (1993).
14. E. Gullikson, "X-ray interactions with matter," The Center for X-Ray Optics, (1995–2010), http://www.cxro.lbl.gov/.
15. J. F. Seely et al., "Coated photodiode technique for the determination of the optical constants of reactive elements: La and Tb," *Proc. SPIE* **6317**, 63170T (2006).
16. M. Fernández-Perea et al., "Optical constants of electron–beam evaporated boron films in the 6.8–900 eV photon energy range," *J. Opt. Soc. Am. A* **24**(12), 3800–3807 (2007).
17. R. Soufli et al., "Optical constants of magnetron–sputtered boron carbide thin films from photoabsorption data in the range 30 to 770 eV," *Appl. Opt.* **47**(25), 4633–4639 (2008).
18. G. Monac et al., "Optical constants in the EUV Soft x-ray (5/152 nm) spectral range of $B_4C$ thin films deposited by different deposition techniques," *Proc. SPIE* **6317**, 631712 (2006).
19. I. A. Makhotkin et al., "Spectral properties of La/B-based multilayer mirrors near the boron K absorption edge," *Opt. Express* **20**(11), 11778–11786 (2012).
20. F. Mauri, N. Vast, and C. J. Pickard, "Atomic structure of icosahedral $B_4C$ boron carbide from a first principles analysis of NMR spectra," *Phys. Rev. Lett.* **87**(8), 085506 (2001).
21. R. Lazzari et al., "Atomic structure and vibrational properties of icosahedral $B_4C$ boron carbide," *Phys. Rev. Lett.* **83**(16), 3230–3233 (1999).
22. D. W. Bullett, "Structure and bonding in crystalline boron and $B_{12}C_3$," *J. Phys. C Solid* **15**(3), 415 (1982).
23. S. Koun et al., "Infrared study of amorphous $B_{1-x}C_x$ films," *J. Appl. Phys.* **78**(5), 3392–3400 (1995).
24. I. Jiménez et al., "Photoemission, X–ray absorption and X–ray emission study of boron carbides," *J. Electron Spectrosc. Relat. Phenom.* **101–103**, 611–615 (1999).
25. F. Scholze et al., "Status of EUV reflectometry at PTB," *Proc. SPIE* **5751**, 749–758 (2005).